Finite Element Analysis of the Direct Shear Test

직접 전단시험의 유한 요소 해석

Yi, Chang－Tok*
이　장　덕

요　지

흙과 Geogrid 사이의 응력 전달은 마찰저항 및 수동저항으로 나눌 수 있는데 Geogrid의 횡방향 요소에 작용하는 수동저항은 그 메카니즘이 복잡하여 아직까지 거동이 명확하게 파악되지 못하고 있다. 이러한 수동저항의 메카니즘을 이해하기 위하여 돌기가 있는 보강재에 대한 직접 전단시험을 유한 요소 방법으로 해석하였다. 유한 요소해석으로 돌기의 간격에 따라 수동저항의 크기, 파괴형태, 응력 및 변형 분포 등을 분석하였으며 이 결과들을 실제 계측치와 비교 분석하여 Geogrid의 횡방향 요소에 작용하는 보강재의 수동 저항의 거동을 파악하도록 하였다. 또한 흙의 종류에 따라 수동저항의 메카니즘을 파악하기 위해 점성토에 작용하는 수동저항의 거동을 예측하였다.

Abstract

The stress transfer mechanism between soil and grid reinforcements involves two basic mechanism: frictional soil resistance and passive soil resistance. However the mechanism of the passive soil resistance is very complex to understand. To study the failure mechanism of ribbed reinforcement, the direct shear tests which are dominated by passive soil resistance are analyzed by using the finite element method. The finite element method is used to examine the effects of ribs on this passive soil resistance development and the mechanism of failure. The calculated behavior of the ribbed reinforcement is compared with the measured behavior. Comparisons between the measured and the simulated strain patterns, failure modes and load-displacement relationship are presented. The behavior of the ribbed reinforcements in a cohesive soil is predicted on the basis of a good agreement between the measured and the predicted behavior of the Ottawa sand.

Keywords : Passive soil resistance, Ribbed reinforcement, Finite element analysis, Direct shear test, Failure surface

* 정회원, (주)파일테크 이사

1. Introduction

In the last two decades a wide variety of reinforcements have been used for civil engineering applications. The economical and safe design of reinforced soil structures requires the knowledge of both the mechanical behavior of the composite material and the behavior at the soil-reinforcement interface. The interaction behavior at the soil-reinforcement interface has been investigated extensively by using various types of geosynthetics in large scale laboratory pull-out and direct shear tests.

The stress transfer mechanism between soil and grid reinforcements involves two basic mechanisms: namely, lateral friction which can be active in nonwoven geotextiles and passive soil resistance on the transverse elements of geogrid. In reinforced soil structures, such as reinforced soil walls and embankments, the primary mechanism of stress transfer is frictional, with passive soil resistance playing an important role when grid reinforcements are employed. However, the relative contribution of each is indeterminate. The displacements require to generate each mechanism can be substantially different and often difficult to determine.

Load transfer between soil and reinforcement by frictional resistance depends on the interface characteristics between the soil and the reinforcements, and the normal stress between them. If the value of the normal stress on the reinforcement is known, it would be a simple matter to calculate the limiting value of the frictional resistance. However, the effective normal stress and the frictional coefficient are altered by the soil-reinforcement interaction and the influence of dilatancy, respectively. Load transfer by passive soil resistance has been considered to be similar to an anchored system consisting of deadmen anchor and ties. There are a number of elements oriented transversely to the pull-out direction each of which develops passive resistance along its front. An individual transverse member alters the state of stress in the region behind it and affects the stress distribution caused by the following members. Therefore, a single anchor system does not behave as a reinforced soil system. Several investigators (Jewell et al., 1984; Heucke and Kwasniewski, 1964) considered the passive resistance on the transverse element of the reinforcement as the bearing capacity of a deep foundation, and introduced a bearing capacity factor to calculate the ultimate passive resistance.

To study the failure mechanism of ribbed reinforcement, Irsyam(1991) performed a series of tests using steel ribs in Ottawa sand. In this paper the direct shear test instrumented in the laboratory by Irsyam(1991) is analyzed by using the finite element method to understand the soil-reinforcement interaction behavior. Since the behavior of this ribbed reinforcements in the direct shear test would be dominated by passive soil resistance, the direct shear tests using the ribbed reinforcement are used to investigate the interface behavior between soil and ribbed steel reinforcements. The finite element method is used to examine the effects of ribs on this passive resistance development and the mechanism of failure adjacent to the ribs. Comparisons between the measured and the simulated strain patterns, failure modes and load-displacemnt relationship are presented and discussed. On the basis of these comparisons, the behavior of the ribbed reinforcement in cohesive soil are also predicted.

2. Experimental Configuration

The shear stress-strain relationship developed along the soil-reinforcement interface is commonly obtained from a direct shear box and/or a pull-out box test. However, no test methods can measure the two mechanisms of the passive soil and the frictional soil resistance independently. The contribution of passive resistance may be affected by several factors: geometry of the reinforcement, stiffness of the reinforcement, density of the soil, grain size, grain shape and normal stress. The geometry of the reinforcement includes major factors such as rib geometry, rib spacing and surface roughness.

The influence of geometry of the reinforcement was reported by Chang et al.(1977) who carried out a pull-out test using a mesh steel reinforcement in sand. The passive soil resistance contributed about 90% of the total pull-out resistance measured. Therefor, it is important that the behavior of the passive resistance be understood for interface modeling in the finite element methods.

The direct shear tests, using ribbed reinforcement, were executed by Irsyam(1991) for the understanding of the behavior of soil particles and the load transfer mechanism between soil and steel ribs. The testing apparatus was a modified direct shear test device having a size of 267mm x 140mm x 76mm high as shown in Fig. 1. This system included an electronic data acquisition system and video camera to view the enlarged intrarib zone on a large monitor. The direct shear box was constructed with Plexiglas walls to facilitate visual observation of grain structure during shearing. Grains of sand were colored to allow movements of select individual grains to be followed and tracked on a large monitor. A carbowax solidification procedure was adopted to verify visual observations, actual measure-

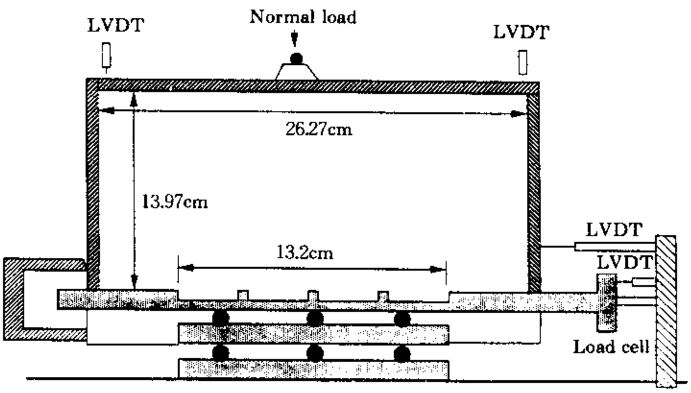

Fig. 1 Direct shear device for ribbed reinforcement testing

ment of void ratio and identification of failure surfaces. The technique utilized hot wax injected through a 0.12cm hole at the base of the ribbed reinforcement. Copper tubes carried out hot water through the plate to prevent wax solidification, and cool water to rapidly solidify the wax. Total shearing resistance was measured by a load cell and the relative horizontal displacement of the plate to the box was recorded by two LVDTs attached to the reaction plate. More detailed description of the technique can be found in Irsyam (1991).

To investigate the effect of rib spacing of the reinforcement on the passive soil resistance, spacings of 0.0, 1.5 and 3.3cm. were used. The experimental work was performed by using Ottawa sand which was categorized as a uniform sand with coefficients of uniformity, Cu between 1.10 and 1.30. A normal stress of 48.3kPa was applied at the top of the loading plate. The tests were conducted by displacement control with a constant rate of base plate displacement.

3. Finite Element Modeling

Irsyam carried out direct shear tests using the ribbed steel reinforcement in Ottawa sands. For a rib height and width of 2.5mm, the spacing was selected to be 3.3cm for dense Ottawa sands which were prepared at a void ratio of 0.51. A normal stress of 48.3kPa was applied on the top plate. Several rib spacings were tested to investigate the effect of rib spacing. If the rib spacing is small, the shear failure surface cannot be completely formed and therefore reduces the overall passive resistance. The rib spacing of 3.3cm, 1.5cm and 0.0cm are chosen for the finite element analysis.

The average grain size (D_{50}) of the Ottawa sand was 0.78mm. When it was compared with the height of rib, 2.5mm, only three times the grain diameter equaled the height of the rib. In practice, the effect of grain size cannot be evaluated by the conventional finite element method but can be studied by using the discrete element method. If the grain size is much larger than the rib size, grains will override the ribs and a passive zone on the shear failure surface will fail to develop. To investigate the behavior of the soil in detail, a fine mesh was used around the bottom of the plate as shown in Fig.5.

The finite element mesh for the shear box test constitutes 684 soil elements and 98 ribbed steel reinforcement elements using a total of 2274 nodes. Soil and reinforcement elements were modeled using a 8 node element. Usually the behavior of the interface between the soil and the reinforcement should be simulated by using an interface element because the relative displacement or shearing would occur between the interface. According to the observed shear failure surface around the ribs after one rib spacing of relative displacement, the failure surface was fully developed immediately above the ribs. Slippage was not observed at the interface between the soil and the reinforcement. For the zero rib spacing case, slippage will be expected between soil and steel. Hence, an interface element should be used to simulate the shearing in the horizontal direction between soil and steel.

The stress-strain relationships of the Ottawa sand could be simulated by the hyperbolic model. Since the triaxial test results of the Ottawa sand with void ratio of 0.51 were not published, the triaxial test results of the Ottawa sand with void ratio of 0.53 carried out by Holubec(1968) were used to obtain the soil parameters. The material parameters were determined on the basis of the laboratory test results which may not provide the best fit of test observations due to different stress path and compaction efforts. Therefore, one needs to calibrate the finite element model using the test measurements. Preliminary material parameters were obtained from laboratory test results and applied to the direct test analysis. Then, the material parameters were changed until the calculated values provide best fit of the load-displacement curves of the direct shear test. It was necessary to simulate the triaxial tests using selected material parameters in order to compare the numerical results with the experimental test results. Fig. 2 shows the predicted stress-strain and volume change curves compared with the laboratory test results. The predicted and measured stress-strain curves would agree well at smaller confining pressures. The material parameters used in simulation of triaxial tests are listed in Table 1.

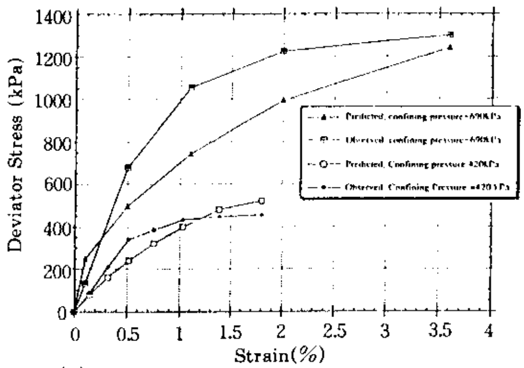

(a) Hyperbolic stress-strain curves compared with the experimental results

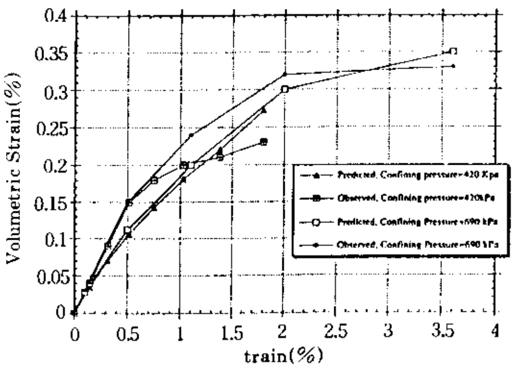

(b) Hyperbolic volumetric strain curves compared with the experimental results

Fig. 2 Hyperbolic model analyses compared with experimental results

Table 1. Soil and steel reinforcement parameters used in analysis

Parameter	Symbol	Ottawa Sand	Steel Plate	Cohesive Soil
Elastic Modulus(kPa)	E		10^9	
Poission's Ratio	υ	0.31	0.28	0.41
Cohesive (kPa)	c	0		25
Modulus Number	K	126		
Modulus Exponent	n	0.85		
Failure Ratio	Rf	0.85		
Bulk Modulus Number	Kb	450		
Bulk Modulus Exponent	m	0.67		
Unit Weight(kN/m^3)	γ	18.9		
D_{50}(mm)		0.72		
Friction Angle(°)	ϕ	34		23

In the hyperbolic mode, the soil modulus is a function of the confining stress. If the confining stress becomes zero or negative, the calculated soil modulus will be incorrect. As the ribbed reinforcement was pulled out, tensile stresses developed around the ribs. In addition, tension zones were formed behind the ribs under small displcements, which gave incorrect stress values due to incorrect stiffness calculation based on the hyperbolic model. To overcome the tension zone problems soil modulu in the tension zone was assigned to a small value, set at 1% of the rebound soil modulus.

In the experiment, shear failure surfaces started to form after a relative displacement of 0.25cm, and completely formed at a rib spacing displacement of 3.3cm. The latter displacement is large compared with the dimensions of the experimental devices. Large displacement problems cannot be dealt with by using a small displacement finite element model. However, as shown in the plot of the shearing resistance against relative displacement in Fig. 3, the relative displacement for peak shearing resistance was small, which can be analyzed by using the small displacement finite element formulation. As the displacement of the reinforcement is increased, the tension zone behind the ribs extended rapidly, which causes numerical difficulties. The maximum total displacement of the reinforcement in the finite element model is 0.3cm after 6 modeling steps. Forces are applied in the numerical model by applying horizontal displacements on the right side of the steel plate.

4. Numerical Results and Discussions

4.1 Shearing Resistance versus Relative Displacement

The main objective of the direct shear test is to obtain shearing force versus relative displacement curves which can be used to evaluate the interaction between soils and reinforcements. Some shearing resistance was mobilized at no relative displacement, which is interpreted to be the frictional resistance between the direct shear box and the roller supporting

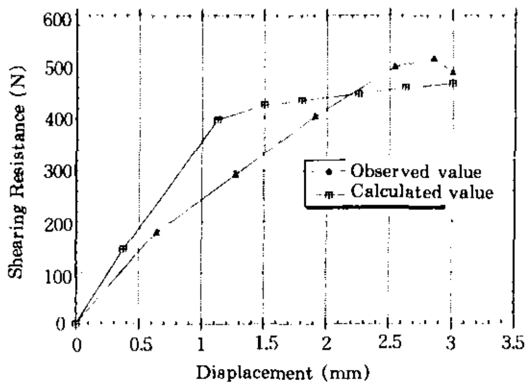

Fig. 3 Measured shearing resistance versus relative displacement compared with calculated values: Rib size=2.5mm, Rib spacing=33mm, Normal Stress=48.3kPa

the testing device. This shearing resistance acting outside the shear box could be neglected because the analysis deals with the behavior inside the shear box and interaction behavior between soil and reinforcement. Therefore, the shear force versus the relative displacement curve was moved to the origin as shown in Fig. 3.

Fig. 3 shows the calculated and observed shearing resistance against relative displacement in the direct shear test. The predicted response gives a good agreement until the relative displacement reaches 0.3cm.

It was observed that there was a zone of relatively high dilation around the ribs and a zone of relatively high shear strain at the top of ribs in the dense sand at small displacement. These zones might be extended as the relative displacement increased: eventually they formed the shear failure surfaces at a relative displacement of 0.25cm.

The steel plate without ribs was also analyzed to evaluate the effect of the ribs by using the same input parameters as the ribbed reinforcement. Shearing occurred at the interface between the soil and plate in this case. The frictional resistance of the steel plate without ribs can be estimated by using a proper shear stiffness of the interface element based on the assumption that the shear failure surface of the steel plate without ribs will develop along the steel plate. This shearing failure surface between the soil and the reinforcement was simulated by using a thin interface four-node quadrilateral interface element which has resistance in compression and in sliding.

The shear and normal stiffness for the interface element were adopted as $5000 kN/m^3$ and $10^{10} kN/m^3$, respectively. Unfortunately, the shear force-displacement curves to determine the shear stiffness for the plate without ribs were not published by Irsyam(1991). The order of the magnitude of the mobilized shear stresses in the interface between the soil and the plate during the shearing depends mainly on the value of the shear stiffness.

Shear forces of the steel plate without ribs contributed the frictional resistance along the reinforcement. The shear failure surfaces of the steel plate without ribs are expected to be different from those of the ribbed plate. Fig. 4 shows the mobilized shear strain at the interface between soil and the steel plate at the relative displacement of 0.3cm. The shear strain of soil is concentrated at the interface between soil and plate and propagated along the interface. This indicates that the sand is sheared along the plate without developing the passive zone, therefore, the shearing resistacne consists of frictional resistance only.

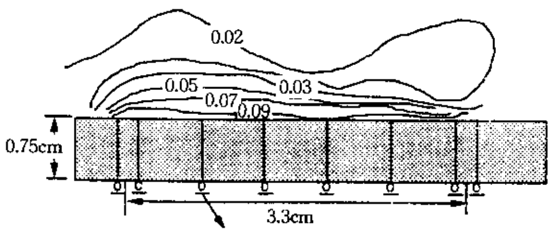

Fig. 4 Shear strain distribution for plate without ribs at displacement of 0.3 cm

The presence of the ribs can significantly change the soil behavior at the interface. To investigate the effect of the rib on the stress at the interface, the nodal point located behind the rib in the center of the plate is selected. Fig. 5 shows the state of stress by the Mohr circle at soil nodal point 294 for the steel plate without ribs and with ribs at the relative displacement of 0.3cm, respectively. For the ribbed steel plate the mobilized shear stress is less than that of the plate without ribs. It is interesting to note that the presence of the ribs can also change the normal strees. As the relative displacement is increased, the soil on the back of the ribs becomes loose, which resulted in the development of a compressive soil arching between the top of the rib and the plate base. This arching effect reduced the normal stress for the ribbed steel plate. Therefore, the presence of the ribs can alter the shear failure surface and the shear resistance.

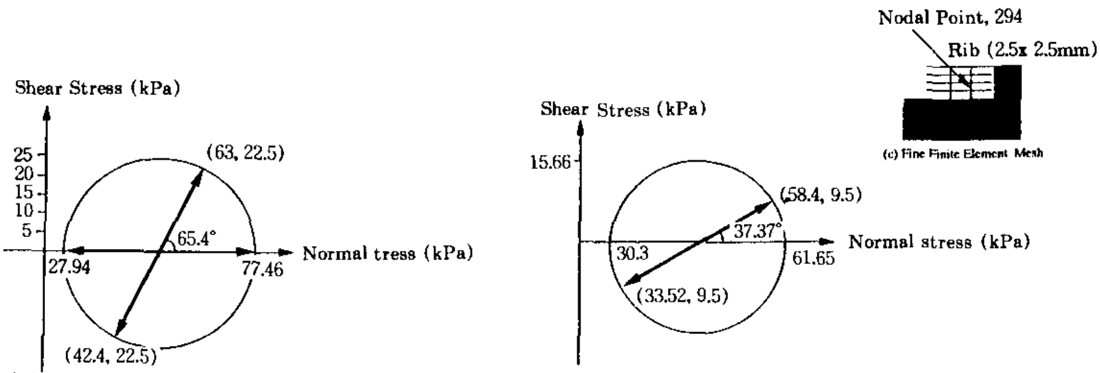

(a) Stress at nodal point 294 for plate without ribs

(b) Stresses at nodal point 294 for ribbed plate

Fig.5 Stress changes at nodal point 294 due to ribs at displacement of 0.3cm

4.2 Shear Failure Surface

The observed failure surface during the shearing process was strongly dependent on the spacing of ribs for a rib height of 2.5mm. For a larger rib spacing of 33mm, a full passive soil wedge was developed at the face of each rib. Although the entire zone between the adjacent ribs could not be captured optically, it was evident that the failure surfaces dipped below the tops of the ribs and in same cased scraped the base of the plate. A typical failure pattern for rib spacing of 33cm was ribs, touched the base plate, and continued to the rear face of the previous rib. For a small rib spacing of 15mm soil grains became trapped between the ribs. The failure surface in such cases was flat, horizontal and immediately above the ribs, which means that for small rib spacing the large portion of the shearing resistance is due to frictional resistance of the soil. Small passive zones could develop for a rib spacing of 1.5cm. The failure surfaces for the 3.3cm and 1.5cm rib spacing were shown in Fig. 6. The frictional resistance developed was partially along a soil-soil interface ans partially along the soil-top of the ribs interface.

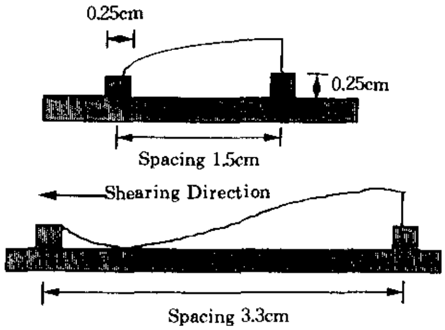

Fig. 6 Effect of rib spacing on failure surfaces (after Irsyam, 1991)

These failure patterns could provide an explanation for the test conducted by Palmeira and Milligan(1989) who varied the spacing of the transverse member of reinforcement in the pull-out test. As the spacing of transverse members decreased, the maximum pull-out resistance became smaller. The contribution of passive resistance to the total shearing resistance was a function of the rib spacing. There might be an optimum spacing of the transverse members for reinforcement for which the passive resistance can be fully developed during the shearing process.

In addition to the 3.3cm rib spacing, a 1.5cm rib spacing is analyzed to investigate the effect of rib spacing on the failure surfaces. The predicted shear failure surface for the 3.3cm rib spacing from the finite element analysis at the relative displacement of 1.2mm is presented in Fig. 7. The Mohr-Coulomb failure criterion was used to determine the failure condition of the soil.

The failure ratio is defined as the ratio of the failure shear stress to the mobilized shear stress. Shear failure surfaces could be determined by a failure ratio of 1. The predicted shear

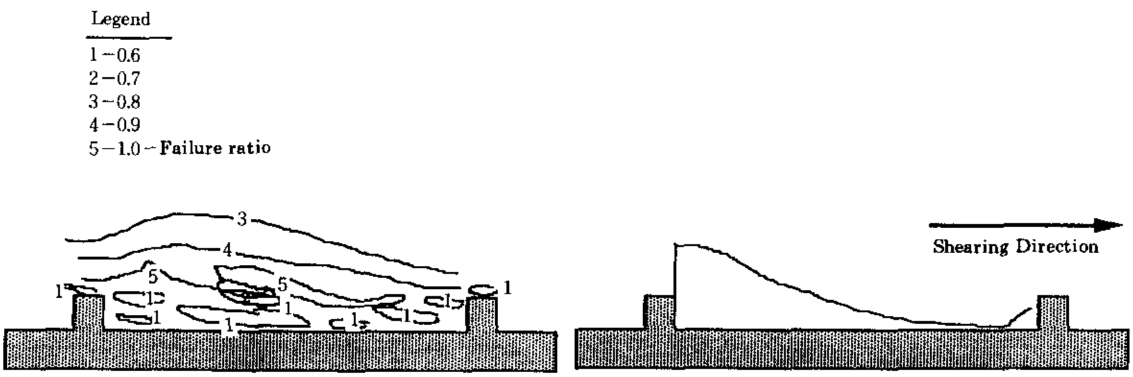

(a) Predicted failure surface, displacement, 1.2mm (b) Observed shear failure surface

Fig. 7 Calculated shear failure surface compared with observed failure surface 3.3 cm rib spacing failure surface was in a good agreement with the observed shear failure surface at the rear part of the failure surface where the passive resistance was considered to be mobilized after a certain displacement. However, in the first part of the shear failure surface where the friction was the dominant resistance, the predicted failure surface formed above the observed one.

According to the observed shear failure surface, the failure surfaces were completely formed at a relative displacement of 2.0cm which corresponds to the residual shearing resistance in the shear force-displacement response. The complete formation of a failure surface might be associated with the establishment of a constant residual shear resistance. However, the shear failure surface started to from at a small relative displacement of 1.0mm, and the peak shearing resistance was reached at a displacement of 2.5mm. Therefore, the predicted shear failure surface at a relative displacement of 1.2mm could reasonably predict the shear failure surfaces. The predicted shear failure surfaces at the center of the ribs are adopted in order to minimize the effect of the wall boundary conditions of the shear box.

To investigate the effect of the rib spacing on the soil behavior around the ribs, the mobilized shear strain is compared in Fig. 8. The shear strain for the 1.5cm rib spacing is highly mobilized above the ribs which corresponds to the shear failure surface. The strain distribution between adjacent ribs is different for both cases. For the 1.5cm rib spacing, the soil between adjacent ribs is trapped and moves together. However, the mobilized shear stress shows similar distributions above the 2.0 rib heights from the plate base, which is not dependent on the rib spacing as shown in Fig. 9. It indicates that the rib spacing can affect the stress distribution between adjacent ribs and for one height of a rib above the top of the rib.

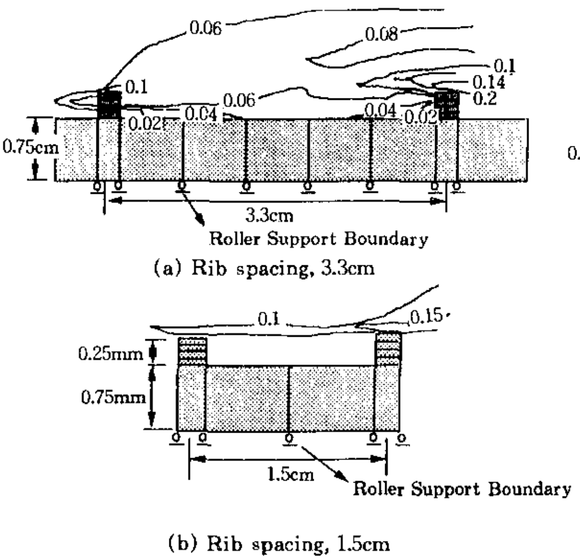

Fig. 8 Shear strain distributions at displacement of 0.3cm

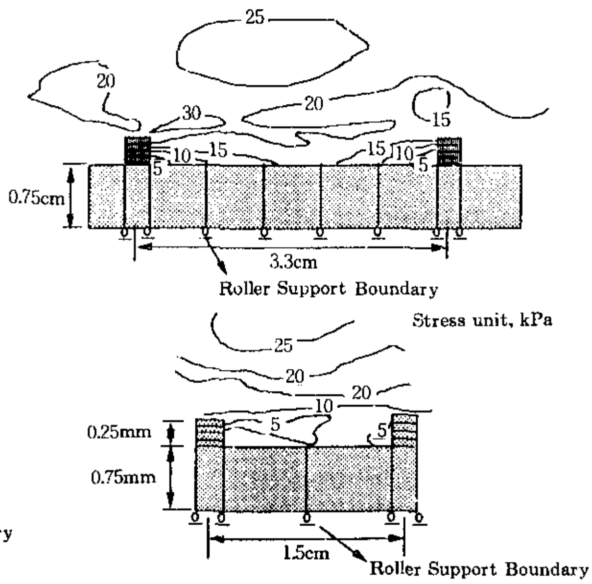

Fig. 9 Shear stress distributions at displacement of 0.3cm

According to the shear failure surfaces for 1.5cm rib spacing, shear forces consist mainly of the frictional resistance due to soil-soil friction and partially of the passive soil resistance for the 1.5cm rib spacing. For the 3.3cm rib spacing, the passive soil resistance is mobilized at the rear part of the failure surface. Therefore, it is expected that the total shear forces for the 3.3cm rib spacing are larger than those for the 1.5cm rib spacing because of the passive soil resistance which can be fully developed for 3.3cm rib spacing. Fig. 10 shows the shearing resistance-relative displacement curves for varying the rib spacing. The contribution of the passive soil resistance to the total shear resistance is a function of rib spacing. Thus, the total shear resistance of the 3.3cm rib spacing is expected to be larger than that of the 1.5cm rib spacing. The total shear resistance at small displacements is identical. As the relative displacement increases, the total resistance for the 3.3cm rib spacing is slightly larger than that of the 1.5cm rib spacing. Usually frictional resistance needs small displacements to be fully mobilized while passive soil resistance requires much larger displacements. Therefore, the frictional resistance for both cases is mobilized at small displacement, which causes the identical shear resistance. However, Fig. 10 shows that after 1.5cm displacement the passive soil resistance starts to mobilize and the total shear force for the 3.3cm rib spacing is increased. The total shear resistance for the 1.5cm rib spacing is mainly due to soil-soil frictional resistance and partially due to the passive soil resistance. As the rib spacing becomes even smaller, the passive soil resistance disappears and the total shear resistance becomes smaller.

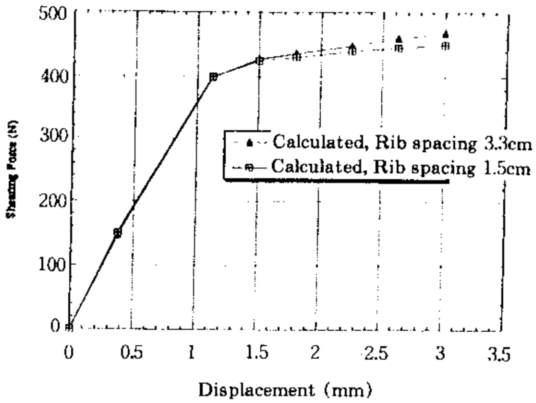

Fig. 10 Effect of rib spacing on shearing resistance

When the typical shear failure surface was compared with the failure modes of the foundation, it was interesting to note that there was much similarity between the two failure modes. Passive soil resistance is developed at the rear part of the failure surface, while the frictional resistance is mobilized at the initial part of the failure surface under small displacements. This indicates that the shear resistance mobilized by friction has reached a maximum; however, the displacement required to mobilize passive resistance is much larger. As a consequence, when both mechanisms are activated it is assumed that the frictional resistance is mobilized at small displacements and the passive soil resistance is predominantly mobilized at large displacements. It is not possible that the frictional resistance is not always completely mobilized before mobilizing the passive soil resistance.

4.3 Shear Zone

The tests were conducted on square ribs with a 3.3cm rib spacing in the dense Ottawa sand. During the first 0.25mm of relative displacement shearing was observed. When shearing began, some grains would be pushed into new positions with little difficulty. The normal stresses acting in the direction of movement were small and the grains evetually took up positions which made further sliding more difficult. Continued shearing beyond the peak stress resulted in continuous loosening of a dilatant soil and a narrow shear zone developed above the ribs. The shear zone thickness changed gradually and grain deformation is localized into a narrower zone after reaching the peak displacement. The zone of limiting equilibrium had expanded to the front and back of the rib which resulted in a longer zone of relatively high shear strain increment which could be viewed as shear failure surface formation.

For a dense sand, continuous shearing changes the void ratio and the thickness of the shear zone. After 0.25cm of relative displacement a failure surface completely formed. Roscoe(1970) stated that the shear zone thickness is a small multiple of the mean grain size. It implies that the thickness of the shear zone is not affected by geometrical dimensions of the soil body. There was ample experimental evidence that shear zones in granular materials involve a significant number of grains(Usegi et al., 1988; Mulhasus and Vardoulakis, 1987; Yoshim and Kishida, 1981). According to Roscoe's experimental observation in direct shear tests the thickness of the shear zone is about 10 times the average grain diameter (D_{50}).

Holtz(1977) conducted pull-out tests on polyester fabric in dry sand at a relative density of 65%, and reported that during the pull-out test high, non-uniform deformation occurred in the fabric. It was observed that the maximum influence zone of the reinforcement was about 10cm on either side of the reinforcement and seemed to be independent of the soil type and confining pressure. Jewell(1980) carried out the pull-out tests in sand using the radiographic technique and several types of reinforecment to investigate the interaction mechanisms. It is interesting to note that the thickness of the shear zone developed adjacent to the reinforcement, as a result of the reinforcement being pulled out, is not strongly dependent on the reinforcement types even though the displacement patterns around the reinforcement vary with reinforcement types.

However, Irsyam(1991) found in this test that the geometry of the ribs has influence on the shear zone thickness. When the trapezoidal ribs were used to investigate the effect of the geometry of the reinforcement, the trapezoidal ribs allowed soil grains to override from the front to the back of the rib. Hence, the trapezoidal ribs behaved merely as a rough surface, which influenced the shear zone thickness. It was found that the shear zone thickness varied from 12 grain diameters to 6 grain diameter at the residual state during the first 0.25cm of a relative displacement.

According to the shear strain distribution in Fig. 8, high shear strain is concentrated at the top of the ribs and it will be extended to form the shear failure surface during the shearing process. Small shear strain occurs between adjacent ribs and at a height of one rib away from the top of ribs. Therefore, it is concluded from the results of the finite element analysis that the shear zone thickness can be expressed in terms of the rib height and at two times the rib height.

4.4 Prediction of Cohesive Soil Behavior

The load transfer and stress distribution between reinforcement and granular soil have been extensively studied in the last two decades. Reinforcement can be used for construction of cost-effective earth structures when poor back fill soils are used for the reinforced soil structures. Therefore, it is necessary to study the load transfer between reinforcements and cohesive soil, especially for the shearing resistance by passive soil resistance on the transverse element of the reinforcement and by combined frictional and passive soil resistance.

As discussed earlier, the direct shear test using a steel plate with ribs and Ottawa sand can be simulated by the finite element analysis. The calculated shear failure surfaces and load-displacement curves give a good agreement with the observed results. Thus the analysis can be extended to the direct shear test using cohesive soil.

The most commonly used characteristics to classify soil are particle size and plasticity. The particle size of soil cannot be simulated by the finite element analysis. The frictional angle of soil is affected by the size of the particle. Generally, clay particles are plate-shaped but granular soil particles are rounded or angular shaped. Therefore, the frictional angle of the soil can be used to indirectly simulate the soil particle size. It was also found from the direct shear test that the effect of particle size was found to be insignificant to the shape of the failure surface for the particles smaller than Ottawa sand(Irsyam, 1991). The plasticity of soil can be simulated by providing the soil cohesion. To compare the analysis results with the calculated results in Ottawa sand, the input data listed in Table 1 are used with the exception of the friction angle and cohesion of the soil. The friction angle of cohesive soil of 23° and cohesion of 25kPa are used for the total stress analysis.

The relationship between shear force and relative displacement is almost the same as the calculated response for the 3.3cm rib spacing. The mobilized shear strain is concentrated at the top of the ribs and propagated parallel to the top of the ribs as shown in Fig. 11. The magnitude of shear strain is smaller than that of Ottawa sand at a relative displacement of 1.3cm. The sheared zone for the cohesive soil is narrower than that of Ottawa sand. It is found that the distributions of shear stress for the cohesive soil is different from that of the Ottawa sand, This implies that the thickness of shear zone is affected by soil types.

The shear zone thickness of the cohesive soil is about 1.5 times the rib height on the basis of the shear stress and strain distributions.

For the Ottawa sand, the shear failure surfaces have close similarity with the local shear failure mode of the foundation. Fig. 12 shows the failure surface of the cohesive soil. The shear failure surface is developed parallel to the top of the ribs. However, it is different from the shear failure surfaces for the 1.5cm rib spacing in Ottawa sand which is formed above the ribs. A large relative displacement of 0.6cm is needed to form the shear failure surface. When compared with the failure mode of the foundation, the shear failure surface is closer to the punching shear failure mode rather than the local shear failure mode.

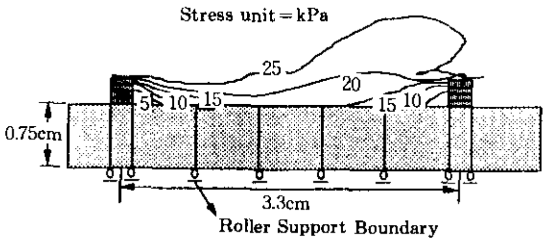

(a) Shear stress distributions

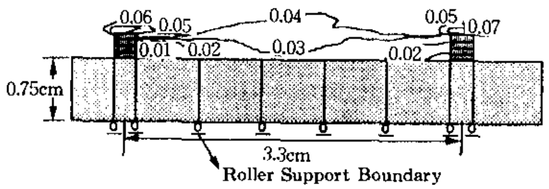

(b) Shear strain distributions

Fig. 11 Analysis of ribbed reinforcement in cohesive soil

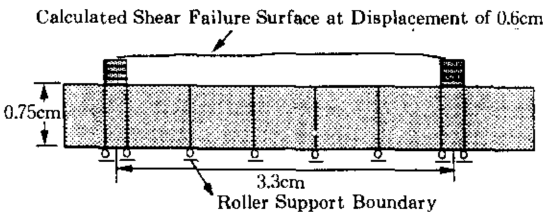

Fig.12 Calculated shear failure surface at displacement of 0.5cm for cohesive soil

5. Conclusion

The main objective of this study is to investigate soil-ribbed reinforcement interaction. The calculated behavior of the ribbed reinforcement is compared with the measured behavior. Based on the comparison conducted and discussed herein, it may be concluded that.

(a) The contribution of passive soil resistance to the total shearing resistance is a function of the rib spacing. As the spacing of the ribs decreases, shear resistance consists mainly of the frictional resistance due to soil-soil friction. There might be an optimum spacing of the transverse member of a geogrid reinforcement at which the passive resistance can be fully developed.

(b) The presence of the ribs in the reinforcement causes shearing resistance to increase and alters the behavior of particles which cause shear failure to form within the soil mass.

(c) The thickness of the shear zone developed adjacent to the ribbed reinforcement can be expressed in terms of the rib height in the numerical analysis and at two times the rib height.

(d) The failure mode of the ribbed reinforcement can be affected by soil type. The sheared zone for the cohesive soil is narrower than that of granular soul. The local failure mode of the foundation is quite similar to the failure mode of the ribbed reinforcement in granular soil. The punching shear failure mode occurs with cohesive soil.

References

1. Chang, J.C., Hannon, J.B. and Forsyth, R.A. (1977) "Pull-out Resistance and Interaction of Earthwork Reinforcement and Soil", Transportation Research Board Record 640, National Research Council Washington, D.C.
2. Duncan, J.M., Byrne, P.,Wong, K. and Mabry, P.(1980) "Strenghth, Stress-Strain and Bulk Modulus Parameters for Finite Element Analysis of Stresses and Movements in Soil Masses", University of California, Berkeley, Report No. UCB/GT/80-01.
3. Holtz, R.D.(1977) "Laboratory Studies of Reinforced Earth Using a Woven Polyester Fabric," Proceedings of the International Conference on the Use of fabrics in Geotechnics, Paris, Vol.3, pp.149-154.
4. Holubec, I.(1968) "Elastic Behavior of Cohesionless Soil", Journal of the Soil Mechanics and Foundation Division, ASCE, Vol.94, No, SM6, pp. 1215-1231.
5. Huecke, S.M. and Kwasniewski J.(1961) "Scale Model Tests on the Anchorage Values of Various Elements Buried in Sand", Proc. 5th International Conference on Soil Mechanics and Foundation Engineering, Paris, Vol. 2, pp. 431-434.
6. Irsyam, M.(1991) The Mechanical Interaction between Cohesionless Soil and Ribbed Inclusions, Ph. D. thesis, The University of Michigan, p.195
7. Jewell, R.A.(1980) Some effects of Reinforcement on the Mechanical Behavior of Soil, Ph.D. thesis Cambridge University
8. Jewell, R.A., Milligan, G.W.E., Sarsby, R.W. and Dubois, D.(1984) "Interaction between Soil and Geogrids", Proceedings of Symposium on Polymer Grid Reinforcement in Civil Engineering, London, England, pp.18-30
9. Mulhaus, H.B. and Vardoulakis, I.(1987) "The Thickness of Shear Bands in Granular Materials", Geotechnique, Vol. 37, No.3, pp.271-283.
10. Palmeira, E.M., Milligan, G.W.E.(1989) "Scale and Other Factors Affecting the Results of Pull-out Tests of Grids Buried in Sand," Geotechnique 39, No.3, pp.511-524
11. Roscoe, K.H.(1970) "The Influence of Strains in Soil Mechanics", Geotechnique, Vol.20, No.2, pp.129-170.
12. Uesugi, M., Kishida, H. and Tsubakihara, Y.(1988) "Behavior of Sand Particles in Sand-Steel Friction" Japanese Society of Soil Mechanics and Foundation Engineering,

Vol.28, No.1, pp.107-118.
13. Yoshimi, Y. and Kishida, H.(1981) "Friction between Sand and Metal Surface", 10th International Conference on Soil Mechanics and Foundation Engineering, Vol.1, pp.831-834.

(접수일자 1996.1.5)